Influence of compressive biaxial strain on the hydrogen uptake of ultrathin single-crystal vanadium layers

G. Andersson, B. Hjörvarsson, and P. Isberg
Department of Physics, Uppsala University, Box 530, S-751 21 Uppsala, Sweden
(Received 12 August 1996; revised manuscript received 24 September 1996)

We have investigated the influence of biaxial compressive strain on the thermodynamic properties of hydrogen in thin, single-crystal vanadium layers (0.9, 1.6, and 2.0 nm). At H/V$<$0.1 (atomic ratio), the host-mediated H-H interaction was found to be attractive. For H/V$>$0.1, the interaction was found to be extremely weak in the 0.9-nm-thick layer and repulsive in the 1.6- and 2.0-nm-thick V layers. The repulsive interaction was found to increase with increasing layer thicknesses. These results are unexpected as the interaction is attractive in both bulk V and in thin vanadium layers under biaxial tensile strain for H/V$<$0.5. Both the strained and unstrained vanadium lattices are found to have roughly the same hydrogen affinity at H/V$=$0.1 (0.3 eV/H). No ordered bulklike β phase was observed at any concentration (0$<$H/V$\leq$1) in the temperature range 30–250 °C. Methods used in this study are resistivity measurements, x-ray diffraction, and nuclear reaction analysis. [S0163-1829(97)02003-1]

I. INTRODUCTION

The effects of boundary conditions and reduced dimensionality on the hydrogen uptake of metals have only recently begun to be the subject of experimental investigations. Alefeld treated the influence of changed boundary conditions on the H-H interaction in a metal-hydrogen system theoretically,[1] but experimental activity has, until recently, been scarce. The hydrogen uptake of epitaxial, clamped Nb films (32–527 nm) was investigated by Song *et al.*[2] In that work the authors showed that boundaries play a major role for films as thick as 100 nm. The phase boundaries are shifted and the critical temperature for the order-disorder phase transition is found to be strongly reduced with decreasing film thickness.

To our knowledge, the only thorough investigation of basic thermodynamic properties of hydrogen in extremely thin hydrogen absorbing layers is that performed by Stillesjö *et al.*[3] on hydrogen in Mo/V(001) superlattices. The effective potential seen by the hydrogen atoms in a Mo/V superlattice is strongly modulated, and the hydrogen is exclusively found in the vanadium layers. This material combination therefore gives rise to a one-dimensional modulation of the hydrogen concentration. The thicknesses of the hydrogen absorbing layer were 1.5 and 2.1 nm, respectively, which correspond to five and seven unit cells of vanadium. An example of a weakly modulated potential is a Nb/Ta superlattice (see, e.g. Ref. 4 and references therein).

In one important aspect, the Mo/V and Fe/V superlattice systems are similar: neither Mo nor Fe will dissolve hydrogen, the heat of solution being endothermic for both metals ($+$0.48 eV/H atom for Mo,[3] and $+$0.30 eV/H atom for Fe (Ref. 5). The hydrogen concentration modulation perpendicular to the film will therefore be one dimensional in a Fe/V superlattice, as in Mo/V.

The interaction of hydrogen atoms in a strongly modulated potential is to first approximation limited to within each minimum. In other words, the hydrogen atoms in one vanadium layer do not interact with hydrogen atoms in the adjacent layers. If the individual V layers are thin enough, they will constitute a quasi-two-dimensional metal host for hydrogen, as in the Mo/V(001) superlattices.[3] Therefore, investigations of hydrogen in the Fe/V superlattice system should render valuable contributions to the knowledge of the influence of boundary conditions and strain on the thermodynamic properties of the V-H system. The use of superlattices as a host opens up a way of investigating the properties of hydrogen in extremely thin films, as the strain state can be altered by proper selection of the hydrogen free layer. The lattice parameter of Mo is larger than that of V, and therefore the vanadium layers are under tensile biaxial strain in epitaxial Mo/V superlattices. In epitaxially grown Fe/V(001) superlattices, on the other hand, vanadium has the larger lattice parameter, with a lattice mismatch between Fe and V of 5.1%. Thus the in-plane, biaxial strain of the V layers is compressive. Within the linear elasticity approach, the biaxial strain state is expected to scale linearly with the ratio of the constituents' thicknesses.

Previous studies of Fe/V multilayers have only concerned magnetic and structural properties.[6] Until recently, the Fe/V multilayers grown have usually been polycrystalline with {110} texture and alloy regions at each interface. However, recently some other groups have been able to grow Fe/V epitaxially,[7,8] hence making samples entitled to be called superlattices. The Fe/V(001) samples used in this study were all epitaxial, single-crystal superlattices.[9]

II. EXPERIMENTAL DETAILS

The Fe/V superlattices were prepared by dc magnetron sputtering onto polished MgO(001) substrates (10×10 mm^2) at 330 °C, and with an Ar gas pressure of 5×10^{-3} torr (1 torr$=$133 Pa). The sputtering equipment and the epitaxial growth of the Fe/V system are described in detail elsewhere.[9]

Samples of three different wavelengths ($\Lambda=L_{\mathrm{Fe}}+L_{\mathrm{V}}$) were grown: $\Lambda=1.8$, 3.2, and 4.0 nm. They were all symmetric, i.e., $L_{\mathrm{V}}=L_{\mathrm{Fe}}=\Lambda/2$. The samples for the resistivity

measurements were covered with a thin (5 nm) Pd layer, to prevent oxidation and facilitate hydrogen loading, while those for concentration measurements were covered by 10-nm polycrystalline V for reasons discussed below. The samples were characterized by low- and high-angle x-ray diffraction (XRD), which showed that the superlattices were of high crystalline quality with a small interface roughness (on the order of 0.2 nm). The resistivity of each sample was measured at room temperature before cutting off a 2-mm-wide strip for the following measurements. A typical resistivity value was 56.3 $\mu\Omega$ cm for a sample with $L_V=1.6$ nm.

The gas system in which the four-point resistivity measurements were performed has been described in some detail elsewhere.[3] In the measurements presented here, hydrogen pressures in the range 0–6000 torr (0–800 kPa) were used, and the temperature was varied between 30 and 250 °C. Above 250 °C the Pd cap layer becomes roughened, which could affect the kinetics of the hydrogen uptake. However, the Fe/V superlattice in itself is thermally stable up to 340 °C.[9]

The applied ac current was 50 μA (corresponding to roughly 25 A/cm^2), which gave a voltage drop of 0.2–1.1 mV over the sensing contacts. This voltage drop was registered by a Stanford Research 830 DSP lock-in amplifier (resolution 0.1% of full scale). Hydrogen pressures were measured with two CCM capacitive pressure gauges with 0–760- and 0–7600-torr pressure spans, respectively, with an accuracy of 0.1% of reading. The base pressure in the system was 3×10^{-8} torr, and the residual gas consisted mainly of hydrogen, with a partial pressure of other impurities in the 10^{-11}-torr region.

After the sample was mounted and the cell evacuated, the temperature was raised to 250 °C, and the sample was flushed several times with pure H_2 to remove water from the chamber walls and oxygen from the sample surface. When the voltage reading was stabilized, the series of measurements was started.

At each temperature (250, 200, 150, 100, 65, and 30 °C) the hydrogen pressure was raised in steps up to a maximum pressure of 6000 torr. The allowed equilibration time at each step was 5–20 min, depending on temperature and pressure. After the last pressure increase the system was evacuated, and the voltage was monitored to see whether the hydrogen loading was reversible. If so, the voltage drop over the sample was the same before and after hydrogenation. The temperature was then lowered to the next value of interest.

The change in resistivity upon hydrogen loading was related to the hydrogen concentration in the V layers by the following procedure. First we loaded V-capped Fe/V samples with hydrogen and measured the change in resistivity simultaneously. When equilibrium was reached after 50–100 h, the samples were cooled down quickly to room temperature, and removed from the hydrogen reactor. Due to the V capping layer, the amount of hydrogen in the superlattice is not affected during the cooling, as the kinetics are extremely slow. After exposure to air, the kinetics are still slower, due to formation of oxides and hydroxyl complexes at the surface. The samples were hydrogenated at selected temperatures and pressures, to give a range of concentrations as wide as possible. The samples were analyzed by x-ray diffraction prior to the hydrogen concentration determination, where the $^1H(^{15}N,\alpha\gamma)^{12}C$ nuclear resonance reaction[10] was used. The annealing at 250 °C was not sufficient to activate the V surface completely, but this was of no concern as the slow kinetics ensured accurate determination of the relation between the concentration and the change in resistivity.

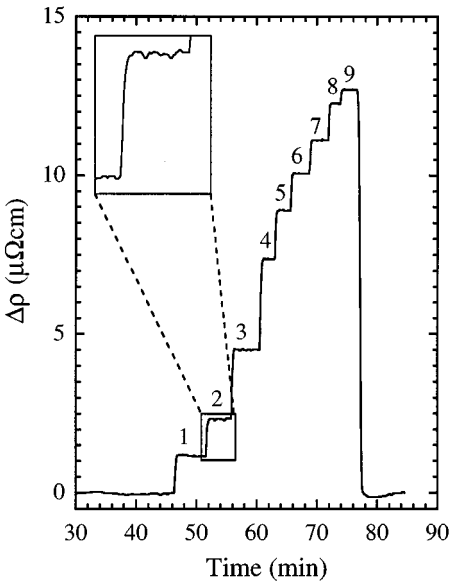

FIG. 1. Example of a hydrogen loading curve, measured at 100 °C. The pressure is increased in steps: (1) 4.1 torr, (2) 7.4 torr, (3) 14 torr, (4) 38 torr, (5) 77 torr, (6) 154 torr, (7) 295 torr, (8) 578 torr, and (9) 731 torr. The inset is an enlargement of step (2).

III. RESULTS

In Fig. 1, a typical example of the resistivity change upon raising the hydrogen pressure is shown. The resistivity returns to its original value as the hydrogen is desorbed from the sample when the reactor is evacuated. Thus the change in the resistivity is found to be completely reversible. Consequently, the hydrogen-induced changes in the sample can be assumed to be reversible. The structural reversibility was investigated by x-ray-diffraction measurements. In Fig. 2, XRD spectra of one of the calibration samples ($L_V=2.0$ nm) before and after hydrogen loading are shown. The XRD measurement was repeated after desorbing the hydrogen, and the resulting diffractogram was found to be identical to the virgin one (within the experimental uncertainties). The bottom spectrum shows that the only noticeable structural change is an out-of-plane expansion of the lattice. At this particular concentration, the expansion of the V layers is approximately 5%. Detailed investigations of the hydrogen-induced lattice expansion in Fe/V(001) superlattices are reported in Ref. 11.

The average hydrogen concentration $\langle H/M\rangle$ in the calibration samples was determined by nuclear reaction analysis.[10] To obtain the average hydrogen content of the V layers is straightforward, using the following relation:[12]

$$c\equiv\left\langle\frac{H}{V}\right\rangle=\frac{L_V+L_{Fe}}{L_V}\left\langle\frac{H}{M}\right\rangle \tag{1}$$

From the results of the calibration measurements the relation between $\Delta\rho/\rho_{20\,°C}$ and c was established. The resulting cali-

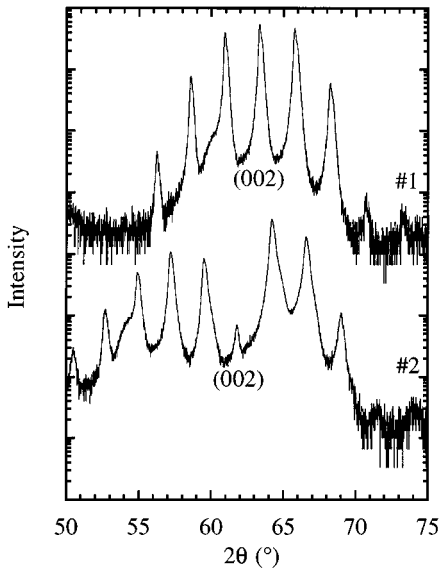

FIG. 2. XRD spectra of a $L_V=2.0$-nm calibration sample before (No. 1) and after (No. 2) hydrogenation at 200 °C, 825-torr H_2. The clearly visible hump to the left of one of the satellite peaks is the signal from the V cover layer. The structural changes are further discussed in Ref. 11.

bration is shown in Fig. 3, where the results are fitted by the following function:

$$\frac{\Delta\rho}{\rho_{20\,^\circ\mathrm{C}}}=Ac\left(1-\frac{A}{B}\,c\right)\quad c\equiv\langle \mathrm{H/V}\rangle \text{ (atomic ratio)}, \quad (2)$$

which is a truncated power series expansion. The particular form for the coefficients was obtained from demanding that the maximum value of $\Delta\rho/\rho_{20\,^\circ\mathrm{C}}$ should agree with that observed in the measurements [maximum of $\Delta\rho/\rho_{20\,^\circ\mathrm{C}}=0.320(1)$ for all three wavelengths]. The values of A and B obtained were 1.07(9) and 1.280(4), respectively. This relation was used to draw the pressure-composition isotherms, shown in Fig. 4(a) for $L_V=1.6$ nm and in Fig. 4(b) for $L_V=0.9$ nm. No deflection point in the resistivity, like the one found in bulk vanadium and Mo/V superlattices at H/V $=0.5$, was observed.

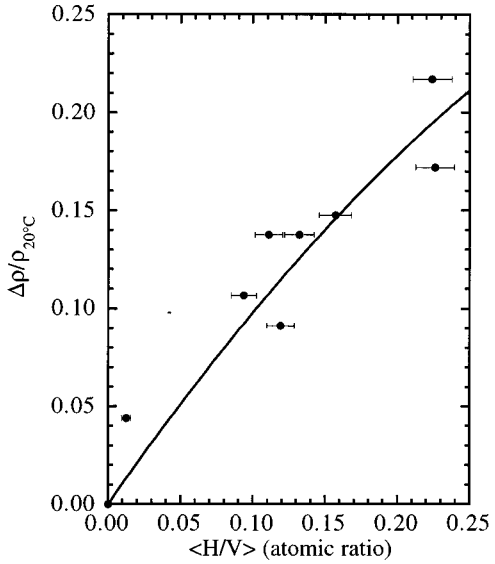

FIG. 3. Calibration of the average hydrogen concentration, valid for all wavelengths. The line is a fit to the function given in Eq. (2).

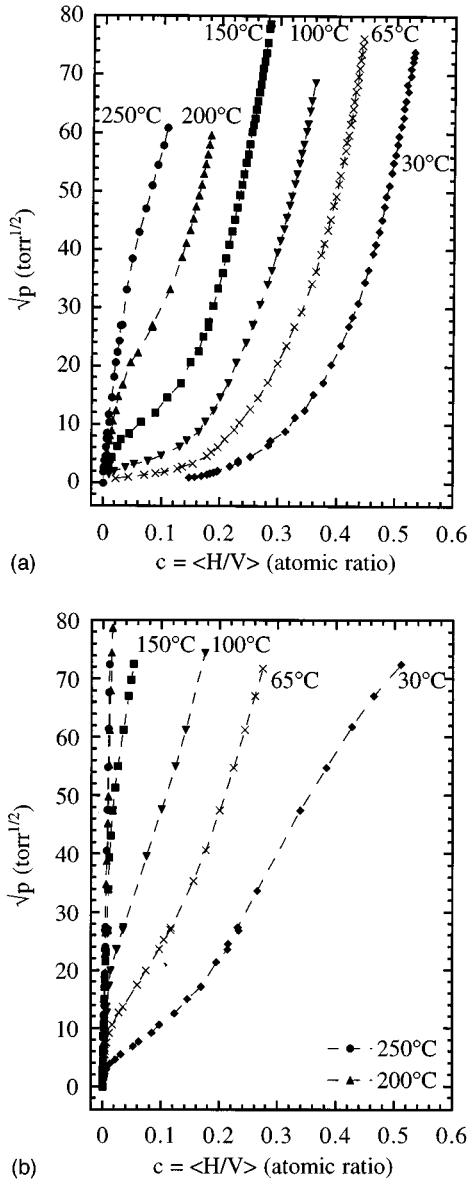

FIG. 4. (a) Pressure vs average composition at different temperatures for the $L_V=1.6$-nm sample. (b) The corresponding data for the $L_V=0.9$ nm sample.

The resistivity of the superlattices can be expressed as

$$\rho=\rho_{\mathrm{H}}+\rho_{\mathrm{phonons}}+\rho_{\mathrm{interfaces}}+\rho_{\mathrm{defects}}+\rho_{\mathrm{others}}, \quad (3)$$

where the four dominating terms are the scattering from the hydrogen atoms, phonons, interfaces, and defects, respectively. The observed scattering of $\Delta\rho/\rho_{20\,^\circ\mathrm{C}}$ is most probably due to variations in the defect density and the interface quality between the different samples. In the calibration $\Delta\rho=\rho_{\mathrm{H}}$ was assumed. The hydrogen density did not affect the temperature dependence of the resistivity, as observed for bulk vanadium.[13]

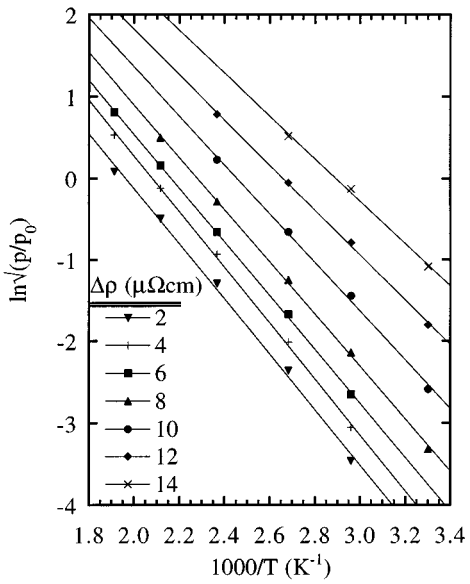

FIG. 5. A selection of van't Hoff plots for the $L_V=1.6$ nm sample. The excess resistivity $\Delta\rho$ is a function of the average hydrogen concentration.

To determine the changes in enthalpy and entropy of solution as functions of hydrogen concentration, van't Hoff plots were made for constant values of $\Delta\rho$. A selection of these plots, for $L_V=1.6$ nm, is shown in Fig. 5. The van't Hoff plots were fitted by

$$\tfrac{1}{2}\ln\frac{p}{p_0}=\frac{\Delta\overline{H}_H}{k_BT}-\frac{\Delta\overline{S}_H}{k_B}. \tag{4}$$

Here p is the hydrogen pressure, p_0 the reference pressure (760 torr), T the temperature in K, ΔH_H the enthalpy change and ΔS_H the entropy change with respect to the gas phase. The values of ΔH_H and ΔS_H do not depend on whether one chooses to use constant $\Delta\rho$ or constant c for the van't Hoff plots.

The solubility in the $L_V=0.9$ nm samples was observed to be considerably lower than for the other two wavelengths. Thus it was motivated to investigate if there were any interface effects of the kind found in Mo/V(001) superlattices.[12,14] The existence of ''dead layers'' at the interfaces will affect the concentration determination, as the extension of these can be comparable to the thickness of the V layers. For this purpose, a multilayered superlattice (MLSL) was grown, with three wavelengths ($\Lambda=4.4$, 3.1, and 1.8 nm, $L_{Fe}=L_V$) matching as closely as possible an integer number of the bct unit cells. In this way one ensures identical conditions for all wavelengths during and after hydrogenation, as the subsamples must be in thermodynamic equilibrium.

In Fig. 6, x-ray-diffraction spectra for this sample before and after hydrogenation are displayed. These show that the structural quality of the sample is indeed high, as the peaks are sharp and well defined. An additional XRD measurement was performed after unloading the sample. The hydrogenation process was found to be reversible, as the structure remained unaltered by the hydrogen cycling. The FWHM (full width at half maximum) of both the θ-2θ scan and the rocking scan (ω scan) retained their original values.

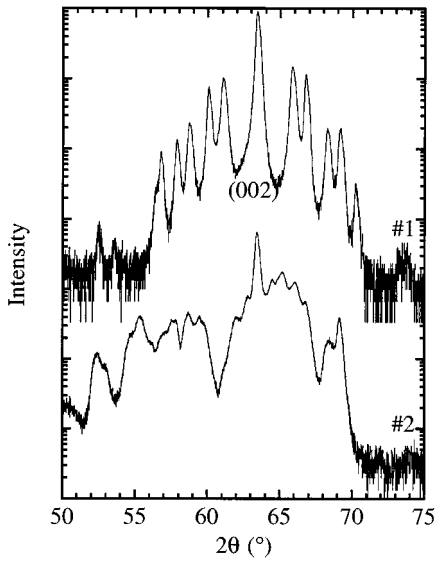

FIG. 6. XRD of the MLSL before (No. 1) and after (No. 2) hydrogenation. The position of the (002) Bragg peak for the unhydrogenated sample gives the average out-of-plane lattice parameter, which is identical for the three wavelengths.

A hydrogen depth profile of the MLSL is shown in Fig. 7, and in Fig. 8 the average H/V atomic ratio is plotted versus $1/L_V$. The intersection of the linear fit with the $1/L_V$ axis, i.e., the V layer thickness at which the hydrogen concentration is zero, gives the extent of the interface region. This was found to be approximately 0.45 nm, or 3 ML of V. When $1/L_V$ approaches zero, the intersection with the y axis gives the concentration in the interior region of the V layers, as the weight of the interfaces becomes negligible. For a further discussion on these phenomena, see Refs. 12 and 14.

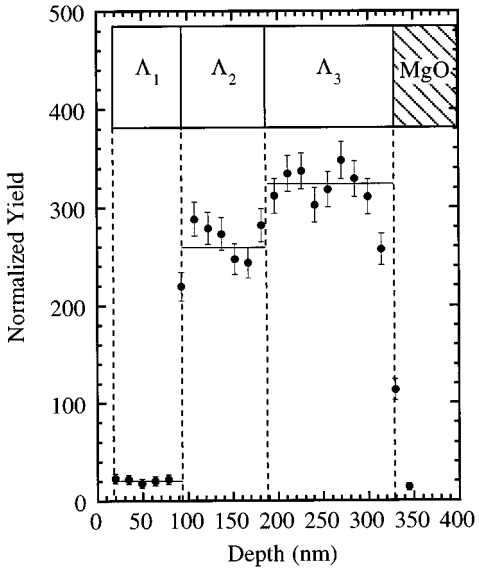

FIG. 7. Hydrogen depth profile for the MLSL hydrogenated at 150 °C, 2100-torr H_2. The wavelengths are $\Lambda_1=1.8$ nm, $\Lambda_2=3.1$ nm, and $\Lambda_3=4.4$ nm. The 10-nm V cover layer is not shown. The normalized yield is proportional to $c=\langle H/V\rangle$.

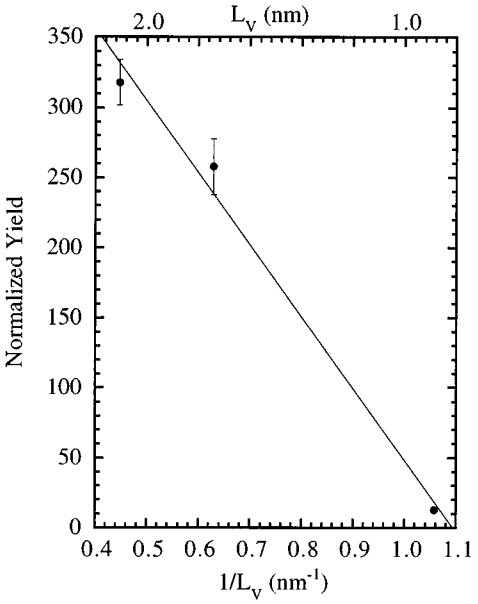

FIG. 8. Normalized yield vs the inverse vanadium layer thickness. The linear fit intercepts the $1/L_V$ axis at a point corresponding to approximately 0.45 nm, or 3 ML.

The fact that three V monolayers at each Fe interface do not dissolve hydrogen to the same extent as the interior region must be taken into account when discussing a concentration dependence of the observables. This as the concentration in the interior region of the V layers is considerably larger than the average concentration. The relation between the interior concentration and the average concentration is

$$c_{\text{interior}}=\frac{L_V}{L_V-2\Delta}\,c, \quad c_{\text{interior}}\equiv\left\langle\frac{H}{V}\right\rangle_{\text{interior}}, \tag{5}$$

where Δ is the thickness (in the same units as L_V) of the interface region. Here we have assumed that the hydrogen content of the interface region is negligible. A correction for the population of the third vanadium layer from the interfaces is straightforward, using a two-level model. This is not considered here, as the correction is only significant at high concentrations. For the shortest wavelength, which in principle consists of an interface region only, the hydrogen atoms can be assumed to be distributed in the two central monolayers. Thus the interior concentration is roughly three times the average H/V in this case.

After this final calibration of the H/V atomic ratio, the ΔH_H and ΔS_H data obtained before were plotted as functions of c_{interior}, see Figs. 9 and 10. In these figures are also shown the corresponding data for the Mo/V(001) system[3] and bulk vanadium.[15–17]

IV. DISCUSSION

It should be emphasized that the values of $\Delta\overline{H}_H$ and $\Delta\overline{S}_H$ do not depend on the determination of the relation between $\Delta\rho$ and c. The only influence of the uncertainty in the concentration calibration is a shift in the scale in H/V. The maximum error in the concentration scaling is 10%. This originates in the uncertainty of the hydrogen concentration

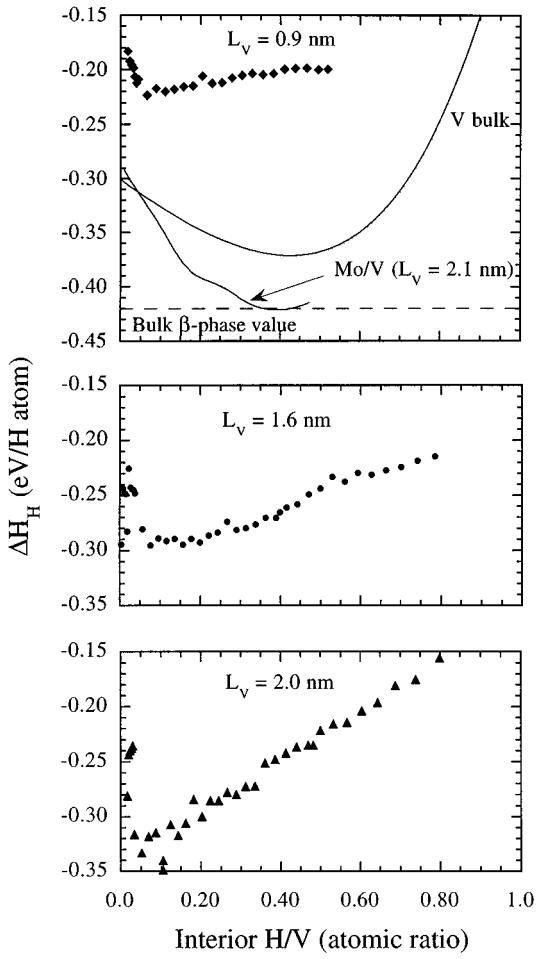

FIG. 9. $\Delta\overline{H}_H$ vs interior H/V atomic ratio. At the top, the results for L_V=0.9 nm are shown together with those for Mo/V (Ref. 3) and bulk V (Ref. 15) [the latter agree quite well with those of Meuffels (Ref. 16)]. The dashed line shows the bulk β-phase value of -0.42 eV/H atom (Ref. 17). The center and bottom plots show the results for L_V=1.6 and 2.0 nm, respectively. The H/V scale has a systematic error of at most 10%.

determination by the $^1H(^{15}N,\alpha\gamma)^{12}C$ nuclear resonance reaction and the scattering in the measured resistivity.

Let us first consider the experimental data with respect to possible phase formation and ordering. The points of inflection of the $\ln(p)$ composition isotherms are commonly accepted as markers of a critical concentration of a phase transition. The only region where inflection points are observed is at low concentrations. For the two longer wavelengths, this critical concentration is independent of temperature and corresponds to an average H/V ratio of roughly 0.09 for L_V=2.0 nm and 0.08 for L_V=1.6 nm. This implies an interior concentration of 0.16 and 0.17, respectively, i.e., approximately one hydrogen per six vanadium atoms. For the shortest wavelength, no reliable information can be obtained at higher temperatures. At lower temperatures however, the critical interior concentration is almost the same as in the other cases (interior H/V$\approx$0.2), but the accuracy of the data is not sufficient to establish any temperature dependence.

In the work on Nb films by Song *et al.*,[2] the slope at the point of inflection (H/Nb around 0.5, atomic ratio) is shown

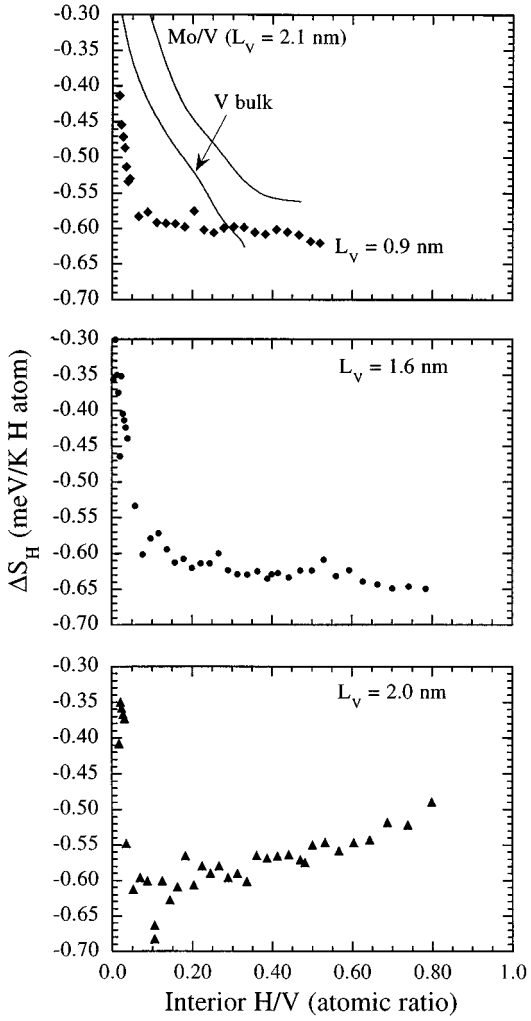

FIG. 10. $\Delta\overline{S_H}$ vs interior H/V atomic ratio. The top plot shows the results for L_V=0.9 nm and the corresponding data for Mo/V (Ref. 3) and bulk V (Ref. 15). The center and bottom plots show the results for L_V=1.6 and 2.0 nm, respectively. The H/V scale has a systematic error of at most 10%.

to obey a Curie-Weiss type of law, i.e.,

$$\left.\frac{\partial(\ln p)}{\partial c}\right|_{[\partial^2(\ln p)/\partial c^2]=0} = \frac{C}{T-T_C}, \tag{6}$$

which is not observed here. The slope at the critical concentration exhibits a minimum at some point in the temperature interval 100–200 °C for the samples with V thicknesses of 1.6 and 2.0 nm. This behavior is observed in bulk VH_x for $x>1$, in the temperature range 0–80 °C and pressures up to 50 bar (5 MPa).[18]

The entropy change (Fig. 10) differs significantly from that observed in the Mo/V and bulk V systems. The decrease from zero is very fast, and then ΔS_H levels out to become almost constant, with the possible exception for L_V=2.0 nm, where there are signs of an increase. This implies less ordering in the longer wavelength at higher concentrations. Still, the degree of ordering is higher than in the Mo/V(001) and bulk V systems. This feature is most likely linked to the reduced number of degrees of freedom in the quasi-two-dimensional host. It is beyond the scope of this article to treat this in any detail.

The hydrogen atoms most likely reside in octahedral O_Z positions in the bct vanadium lattice,[11] even at the lowest concentrations. We do not observe any sign of a transition to a bulklike β phase, although the hydrogen resides in sites characteristic of that phase. This observation implies lowering, or even extinction, of the critical temperature for the bulklike α- to β-phase transition. The absence of the regular β phase is supported by the results from XRD measurements,[11] the absence of a deflection point in $\Delta\rho$, and the constancy of $\Delta\rho_{max}$ at all temperatures. To extend the temperature range further, a V-capped sample with interior H/V=0.24 was slowly cooled to liquid-nitrogen temperature and then allowed to return to 25 °C, while monitoring the resistivity. Ordering of the hydrogen atoms would result in a discontinuity in $\delta\rho/\delta T$,[13] which was not observed.

A. Low concentration limit (H/V<0.1)

The critical concentration is very close to the concentration where ΔH_H has its minimum. Below this concentration, the host mediated H-H interaction is attractive. If we regard the thinnest V layers (0.9 nm), assuming that the H atoms are distributed in the two central monolayers, the conclusion must be that the attractive interaction is within the x-y plane. This behavior is probably connected to the gigantic hydrogen-induced lattice expansion observed at low concentrations.[11] The expansion up to interior H/V≈0.2 was found to be more than three times larger than at high and intermediate concentrations. The change in the effective potential is closely linked to the change in the interstitial electron density. We can easily obtain a rough estimate of this change. The electronic charge associated with the interstitial protons can be assumed to be local compared to the range of the elastic interaction. When the hydrogen content of the sample is increased from 0 to 0.1, the average volume increase of the V layers is 2%. The interstitial electron density is then decreased, and the change in the absorption potential can be estimated within the framework of the effective-medium theory,[12]

$$\delta\Delta E = (796 n_0 + 20.8)\,\delta n_0 \quad \text{(eV)}. \tag{7}$$

With an average interstitial electron density n_0=0.03,[12] a change of 2% in volume results in a 27-meV change of the effective potential. This is in reasonable agreement with the values seen in the plot of ΔH_H for the change in energy, going from zero concentration to interior H/V=0.1. Thus it is probable that the attractive H-H interaction is closely linked to the gigantic volume expansion of the host. Direct interaction is not plausible at these low concentrations.

B. Intermediate and high concentrations

For the shortest wavelength (L_V=0.9 nm), $\Delta\overline{H_H}$ has a much weaker H/V dependence than observed in the thicker vanadium layers at H/V>0.2. The almost constant ΔH_H implies that there is weak interaction between hydrogen atoms within the same (001) plane at interior concentrations above 0.2. The hydrogen is therefore best described as a weakly interacting, two-dimensional gas or liquid at these concentra-

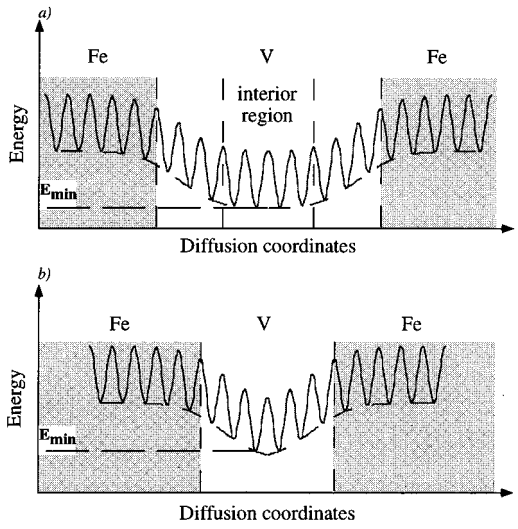

FIG. 11. A schematic view of the potential seen by a diffusing H atom. The shadowed areas are the iron layers surrounding the vanadium, which is (a) 10 ML and (b) 6 ML thick, respectively. In (a) the energy difference between monolayers 3 and 4 from the interface is 97(5) meV. $E_{\min}$ in (b) is 87(6) meV higher than in (a).

tions. In this sample, the vanadium layers do not have an ''interior region.'' The dissolved hydrogen atoms can be assumed to be distributed in the two central vanadium layers, which correspond to the first dead layer in the thicker samples. These two layers are expected to be equally favorable for the hydrogen atoms to reside in. Figure 11 shows a schematic view of the deduced potential, as seen by the hydrogen atoms in the L_V=1.6 and 0.9 nm samples. The two values of $E_{\min}$ differ by 87(6) meV, with the shorter wavelength at the higher energy. This value is the observed difference between ΔH_H for the sample with the shortest wavelength and the average ΔH_H for the other two at interior concentrations of H/V≈0.1. A further confirmation of this observation is obtained from the hydrogen distribution in the multilayered superlattice (see Fig. 7). Boltzmann statistics, applied on a simple two-level model of the third and fourth V monolayers from the interface, results in a 97(5)-meV difference between these energy levels, in good agreement with the difference deduced from the enthalpy changes. As these energy differences are much larger than k_BT for the temperatures used, we do not need to consider any temperature dependence of the enthalpy change in the low concentration limit. The population of the interface region only becomes prominent at high interior concentrations. The increase in the slope of ΔH_H with increasing layer thickness is a clear sign of repulsive H-H interaction, which can be shown using a simple interface model.[12]

A local correlation between H atoms in the z direction is inferred for the two samples with an ''interior region'' (L_V=1.6 and 2.0 nm).[11] This correlation is necessarily limited by the finite size of the V layers, as no higher-order interactions can be mediated by the Fe spacer layer. As there is no deflection point in the resistivity, no long-range correlations are expected in the x-y plane. This conclusion is supported by the temperature independence of the maximum $\Delta\rho$ value reached, as mentioned above.

If we now assume that the hydrogen resides in the same site throughout the concentration range 0.1 to 1, we can conclude that the nearest- and next-nearest neighbor H-H interaction in this concentration range is repulsive, and that the interaction strength increases linearly with the V layer thickness. That the assumption about the site occupancy is reasonable is evident from the structural investigations,[11] which also show that the strain field associated with each hydrogen atom is close to uniaxial.

An ordered, low concentration hydride phase is observed in yttrium.[19] For temperatures up to 130 °C and H/Y below approximately 0.20, a metastable, ordered solid solution denoted the α^* phase is observed instead of the regular, random α phase. The critical concentration for the transition from the α^* to the $(\alpha+\beta)$ region is independent of temperature, as observed for H in the thin V layers. It is plausible to assume that a quasiordered phase is established in the Fe/V samples, similar to the phase observed in Y. The driving force for this phase formation could be the interplay between the long-range attractive interaction and the repulsive short-range interaction.

To summarize the conclusions drawn so far about the phase diagram of hydrogen in the Fe/V samples, there is only one phase transition, at interior H/V≈0.16, in the temperature region 30–250 °C. Below this critical concentration we have the disordered, gaslike α-phase. In a small concentration region in the vicinity of the transition, a short-range ordered α^* phase, as observed in yttrium, is plausible. At higher concentrations (up to H/V≈1), we have a liquidlike phase α'. In this phase the ordering in the planes parallel to the sample surface is of short range, while in the z direction the correlation length is, by necessity, limited by the V-layer thickness. This phase can be described as a ''two-dimensional liquid.''

V. SUMMARY

The solubility and thermodynamics of hydrogen in compressively strained vanadium layers of thicknesses 0.9, 1.6, and 2.0 nm in Fe/V(001) superlattices were studied using a resistometric method. The long-range host-mediated H-H interaction in the plane was found to be attractive. The short-range interaction was discovered to be close to uniaxial in the z direction and repulsive, as seen in the 1.6- and 2.0-nm layers. This behavior is the opposite to that seen in bulk V and thin V layers under tensile strain. The average repulsive interaction was found to increase with increasing thickness of the vanadium layers.

For the thinnest sample in this study, the heat of formation was determined to be −0.18(1) eV/H atom in the infinite dilution limit. The energy difference between hydrogen in 0.9-nm vanadium layers and thicker samples was found to be 87(6) meV/H atom at H/V≈0.1. The only phase transition observed is from the α phase to a liquidlike α' phase, with a possibility of an ordered α^* phase close to this transition. Thus the critical temperature for β-phase formation has been lowered to below at least 25 °C for all concentrations. The triple point between the three phases is above 250 °C.

The $^1H(^{15}N,\alpha\gamma)^{12}C$ nuclear resonance technique was used to probe the concentration variation within a multilayered superlattice. An interface region of 3 ML was inferred. This

interface region does not have the same hydrogen affinity as the interior region of the 1.6- and 2.0-nm-thick V layers. The energy difference between the third and fourth monolayers in V was determined to be 97(5) meV, using a two-level model fitting the nuclear reaction analysis data.

ACKNOWLEDGMENTS

Financial support from the NFR, and from the NUTEK/NFR thin-film growth materials research consortium is gratefully acknowledged.

[1] G. Alefeld, Ber. Bunsenges. Phys. Chem. **76**, 746 (1972).
[2] G. Song, M. Geitz, A. Abromeit, and H. Zabel, Phys. Rev. B (to be published).
[3] F. Stillesjö, S. Ólafsson, P. Isberg, and B. Hjörvarsson, J. Phys. Condens. Matter **7**, 8139 (1995).
[4] P. F. Miceli, H. Zabel, J. A. Dura, and C. P. Flynn, J. Mater. Res. **6**, 964 (1991), and references therein.
[5] R. Griessen and T. Riesterer, in *Hydrogen in Intermetallic Compounds I*, edited by L. Schlapbach, Topics in Applied Physics Vol. 63 (Springer, Berlin, 1988), and references therein.
[6] F. Stillesjö, B. Hjörvarsson, and B. Rodmacq, J. Magn. Magn. Mater. **126**, 102 (1993), and references therein.
[7] M. J. Christensen, R. Feidenhans'l, and M. Nielsen, Vacuum **46**, 1113 (1995).
[8] J. E. Mattson, E. E. Fullerton, C. H. Sowers, and S. D. Bader, J. Vac. Sci. Technol. A **13**, 276 (1995).
[9] P. Isberg, B. Hjörvarsson, R. Wäppling, E. B. Svedberg, and L. Hultman, Vacuum (to be published), and references therein.
[10] W. A. Lanford, Nucl. Instrum. Methods Phys. Res. Sect. B **66**, 65 (1992).
[11] G. Andersson, B. Hjörvarsson, and H. Zabel (unpublished).
[12] B. Hjörvarsson, S. Ólafsson, F. Stillesjö, E. Karlsson, J. Birch, and J.-E. Sundgren, Z. Phys. Chem. **181**, 343 (1993), and references therein.
[13] D. G. Westlake, S. T. Ockers, and W. R. Gray, Metall. Trans. **1**, 1361 (1970).
[14] B. Hjörvarsson, J. Rydén, E. Karlsson, J. Birch, and J.-E. Sundgren, Phys. Rev. B **43**, 6440 (1991).
[15] E. Veleckis and R. K. Edwards, J. Phys. Chem. **73**, 683 (1969).
[16] P. Meuffels, KFA Jülich Report No. Jül-2081, 1986 (unpublished).
[17] T. Schober and H. Wenzl, in *Hydrogen in Metals I*, edited by G. Alefeld and J. Völkl, Topics in Applied Physics Vol. 28 (Springer, Berlin, 1978).
[18] T. Schober, in *Hydrogen Metal Systems I* (Ref. 18), Vols. 49–50, and references therein.
[19] P. Vajda and J. N. Daou, in *Hydrogen Metal Systems I*, edited by F. A. Lewis and A. Aladjem, Solid State Phenomena Vols. 49–50 (Scitec, Zürich, Switzerland, 1996), and references therein.